Asymmetric decision feedback equalizer and full-duplex communication for indoor wireless applications

Égalisateur de décision à contre-réaction asymétrique et communication bidirectionnelle pour des applications de communication sans fil intérieures

K.S. Oler, A.B. Sesay, and B.R. Petersen*

An asymmetric decision feedback equalizer (ADFE) and a full-duplex ADFE system are introduced. The ADFE system achieves a significant asymmetry in the distribution of computational complexity relating to equalization between two transceivers. A mean-square-error analysis is formulated to encompass both the ADFE and the decision feedback equalizer. Both equalizers are shown to have identical characterization and performance under equivalent conditions. The bit error rate of the ADFE is accurately predicted, and error-correlation results are obtained by the use of a finite discrete Markov process. The effects of timing error, adaptive training, mismatch of signal-to-noise ratio and finite precision arithmetic on the performance of the ADFE system are also examined. Transmission is in time-division duplex (TDD) format, and the access technique is time-division multiple access (TDMA). Performance and complexity comparisons are made between the ADFE and the Tomlinson-Harashima precoder with a feedforward filter (TH-FF).

Un égalisateur de décision asymétrique à contre-réaction (ADFE) et un système bidirectionnel sont présentés dans cet article. Le système ADFE permet d'introduire une asymétrie importante de la distribution de complexité algorithmique relative à l'égalisation entre deux transmetteurs. Une analyse par erreur moyenne au carré prenant en compte à la fois l'ADFE et l'égalisateur de décision à rétro-action est présentée. Les deux types d'égalisateurs possèdent des caractéristiques et des performances identiques. Le taux binaire d'erreur de l'ADFE est prédit avec précision et les résultats de corrélation d'erreur sont obtenus par un processus de Markov fini discret. L'effet des erreurs de synchronisation, de l'entraînement adaptatif, de l'incompatibilité du rapport signal sur bruit et de la limitation de la précision arithmétique du système ADFE est également étudié. La transmission adopte le format bidirectionnel en division temporelle (TDD) et la technique d'accès est en accès multiple en division temporelle (TDMA). Une comparaison entre le système ADFE et le système de Tomlinson-Harashima avec pré-codeur et filtre feedforward (TH-FF) au niveau des performances et de la complexité est discutée dans l'article.

I. Introduction

This paper investigates asymmetric equalization of indoor wireless channels. The objective is to facilitate wireless access to wired networks via inexpensive, lightweight portables in work areas. Although multiple portables and base stations are likely in a real system, this paper considers only a single base and portable. The portable communicates with a wired network through a fixed base station. It is also assumed that equalization is required, as is generally the case for indoor wireless communication at rates above 1 Mbit/s [1].

In the target system, the base station is stationary and its size and weight are of little concern. The portable relies on batteries, which contribute to size and weight and require frequent recharging. The size and weight of the portable must be minimized to make it convenient to carry and use, thereby providing greater mobility within a work area (office, lab, and so on). In order to achieve this goal, we propose a system that utilizes an asymmetric decision feedback equalizer (ADFE) in its forward link and a DFE in its reverse link. In asymmetric equalization there is an unequal distribution of equalization complexity through shifts from one transceiver to the other, while effective equalization is maintained in both links.

*K.S. Oler was with TRLabs and the University of Calgary and is now with Cell-Loc, Calgary, Alberta. A.B. Sesay is with TRLabs and the Department of Electrical and Computer Engineering, University of Calgary, Calgary, Alberta T2N 1N4. B.R. Petersen was with TRLabs and the University of Calgary and is now with the University of New Brunswick, Fredericton, N.B. E3B 5A3.

In this work, asymmetry is achieved by using pre-equalization and post-equalization at the base to equalize the forward and reverse links, with little equalization performed at the portable. Data transmission is in time-division duplex (TDD) format, alternating between forward- and reverse-link frames. Both links utilize the same carrier frequency so that the channel impulse responses (CIRs) are identical, according to the principle of reciprocity. The frames are of sufficiently short duration so that the channel changes little over a pair of subsequent frames. Thus, adaptive equalization parameters determined at the beginning of a reverse-link frame would be applicable up to the end of the next forward-link frame.

II. Previous work and results

The term asymmetric signal processing was first applied to the shifting of equalization complexity by Gibbard et al. (the Tomlinson-Harashima precoder with a feedforward filter (TH-FF)) [2]. The reader is cautioned that the term *asymmetry* is used otherwise in the literature as well. For example, it has been used to refer to an imbalance in the I and Q channels [3] or to differing forward/reverse-link data rates [4].

Zhuang et al. [5] propose an asymmetric system employing a linear pre-equalizer and a DFE. Reciprocity is exploited in the characterization of the pre-equalizer. Another system by Zhuang and Huang [6] uses nonlinear phase precoding. However, none of these systems provide adequate performance. Other asymmetric systems have been pro-

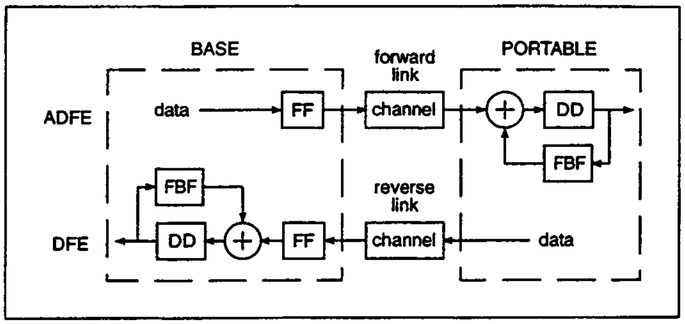

Figure 1: *Basic blocks of an ADFE transceiver.*

posed for line telephone applications, which also exploit reciprocity to characterize the pre-equalizer [7]–[8].

The performance of the TH-FF precoder [2] is close to that of the regular TH precoder [9]–[10], which is also close to that of the DFE. The TH-FF system has been shown to effectively equalize the indoor wireless channel. A high degree of asymmetry is achieved as the only equalization function implemented at the portable is the modulo operation. Reciprocity is exploited by using the DFE parameters to directly characterize the precoder forward filter (FF) and feedback filter (FBF). The TH-FF precoder advantageously shapes the transmitted signal spectrum by reducing power in regions corresponding to spectral nulls in the CIR.

Two drawbacks of the TH-FF system are the significant computational requirements at the base and automatic-gain-control (AGC) sensitivity at the portable. Because the input to the precoder FBF is not quantized, the pre-equalizer requires higher precision than does the DFE. As the FF of the forward link is located at the transmitter, it is unable to adaptively correct for amplitude variations in the received signal. The portable must have very precise AGC so that the effective modulo operator levels are not changed due to scaling of the received signal.

III. Characterization of the ADFE system

An ADFE system for equalizing time-division duplexing communications between a base and portable is shown in Fig. 1. It includes a DFE for the reverse link and an ADFE for the forward link. The ADFE is a DFE with its forward filter located at the transmitter and its feedback filter at the receiver.

A. Model and MMSE characterization of the ADFE

Like the DFE, the minimum mean-square-error (MMSE) characterization of the ADFE requires a suitable model. For convenience, we examine a standard DFE model (Fig. 2(a)) [11] and extend it to the ADFE scheme. The channel has impulse response $\mathbf{h}$, and the input data sequence is $a(n)$. The forward and feedback filters of the DFE are represented by $\mathbf{w}_f$ and $\mathbf{w}_b$, respectively. The synchronization delay between transmitted and detected symbols is denoted by Δ, while the training and estimation error sequences are $d(n)$ and $e(n)$, respectively. The additive Gaussian noise is $v_1(n)$.

If we temporarily assume that the DFE is optimum and has infinite-length FF and that there is no error propagation, then the MMSE is given by (1):

$$J_{\min} = \exp\left\{T_s \int_{-\frac{1}{2T_s}}^{\frac{1}{2T_s}} \ln\left[\frac{N_0}{|H(f)|^2 + N_0}\right] df\right\}, \tag{1}$$

where T_s is the data symbol period, $H(f)$ is the channel transfer function and N_0 is the noise power spectral level.

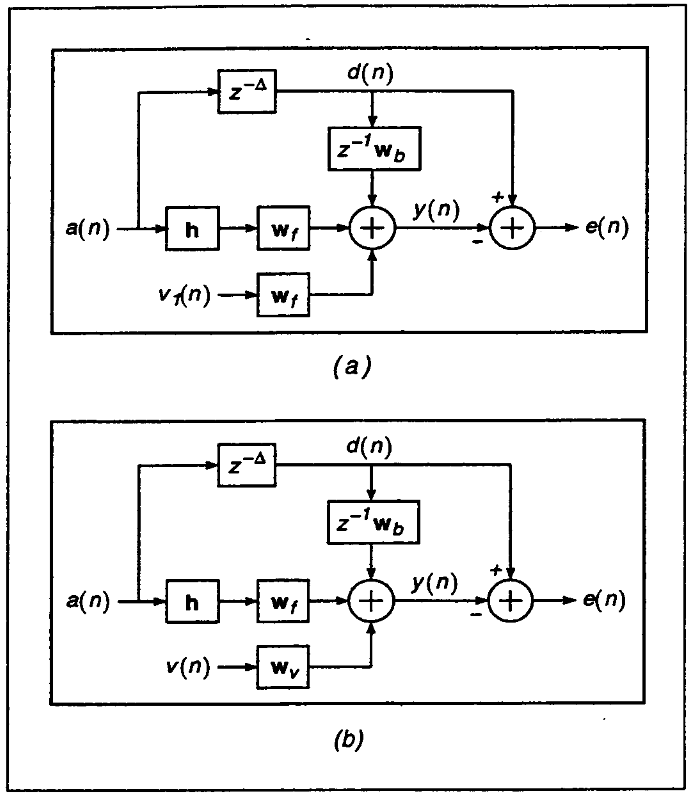

Figure 2: *(a) DFE model without error propagation. (b) A unified DFE/ADFE model.*

The DFE model can be extended to obtain an ADFE model by adding a second noise source, $v_2(n)$, which is not filtered by the forward filter $\mathbf{w}_f$. An ADFE model is attained in the limit as the power in $v_1(n)$ approaches zero, as long as $|H(f)|^2 \neq 0$. The resulting MMSE is indicated by the limit in (2):

$$J_{\min,\mathrm{ADFE}} = E\left[v_2^2(n)\right] + \lim_{N_0 \to 0} \exp\left\{T_s \int_{-\frac{1}{2T_s}}^{\frac{1}{2T_s}} \ln\left[\frac{N_0}{|H(f)|^2 + N_0}\right] df\right\}. \tag{2}$$

The above model is, however, undesirable in that the optimum FF may introduce an arbitrary power gain in the transmitted signal and alter the SNR. The situation may be alleviated by placing a constraint on the transmitted power in the form of a gain factor, K_f, equal to the inverse of the norm of the FF. This gain constrains the transmitted power so that the received SNR is independent of the FF. For analysis purposes only, a corresponding inverse gain is inserted at the receiver so that the magnitude of the equalized signal is approximately equal to that of the desired signal. An AGC circuit would normally perform this function.

A unified model representing an ADFE or DFE is shown in Fig. 2(b), where $\mathbf{w}_v$ shapes the noise input to the decision device and is defined by (3):

$$\mathbf{w}_v = \begin{cases} \mathbf{w}_f & \text{DFE} \\ \left[\sqrt{\mathbf{w}_f^T \mathbf{w}_f} \quad \mathbf{0}_{N_f-1}^T\right] & \text{ADFE} \end{cases}. \tag{3}$$

The MSE analysis for the unified model is applicable to both DFE and ADFE. To derive the MMSE filter weights, we assume that the channel impulse response, $\mathbf{h}$, the forward filter, $\mathbf{w}_f$, and the feedback filter, $\mathbf{w}_b$, are causal with number of taps N_h, N_f and N_b, respectively. For clarity of exposition only, we also assume BPSK data with real signals and filters. Extension to complex signals and filters can be easily made. The variable $a(n)$ is a sequence of equally probable, uncorrelated BPSK symbols. Define the data matrix $\mathbf{A}(n)$ as

$$\mathbf{A}(n) = \begin{bmatrix} a(n) & a(n-1) & \cdots & a(n-N_f+1) \\ a(n-1) & a(n-2) & \cdots & a(n-N_f) \\ \vdots & \vdots & \ddots & \vdots \\ a(n-N_h+1) & a(n-N_h) & \cdots & a(n-N_f-N_h+2) \end{bmatrix}.$$

The desired symbol vector $\mathbf{d}(n)$ is defined as

$$\mathbf{d}(n) = \begin{bmatrix} d(n) & d(n-1) & \cdots & d(n-N_f+1) \end{bmatrix}^T.$$

The additive noise vector, defined as

$$\mathbf{v}(n) = \begin{bmatrix} v(n) & v(n-1) & \cdots & v(n-N_f+1) \end{bmatrix}^T,$$

consists of zero-mean white Gaussian signals with variance σ_v^2. The signal to the input of the decision device is given by (4):

$$y(n) = \mathbf{h}^T \mathbf{A}(n) \mathbf{w}_f + \mathbf{w}_v^T \mathbf{v}(n) + \mathbf{w}_b^T \mathbf{d}(n-1). \tag{4}$$

The MMSE filter weight vector is given by (5):

$$\mathbf{w} = \mathbf{w}_{\text{MMSE}} = \left(\mathbf{R} + \sigma_v^2 \mathbf{D}\right)^{-1} \mathbf{p}, \quad \mathbf{w} = \begin{bmatrix} \mathbf{w}_f \\ \mathbf{w}_b \end{bmatrix}. \tag{5}$$

The diagonal matrix $\mathbf{D}$ and the correlation matrix $\mathbf{R}$ are defined in the Appendix. For identical CIR, synchronization delay, SNR, and number of FF and FBF taps, the DFE and ADFE have identical $\mathbf{w}_{\text{MMSE}}$ and MMSE ($J_{\min}$), where $J_{\min}$ is given by (6):

$$J_{\min} = 1 - \mathbf{w}_{\text{MMSE}}^T \mathbf{p}. \tag{6}$$

The expressions for the MMSE filter weight vector and the resulting MMSE for QPSK modulation are the same as those given by equations (5) and (6) for PSK. The only difference is that, for QPSK, all the vectors involved are complex-valued. This is a consequence of the complex-valued nature of QPSK signals.

In the case of nonoptimal coefficients it can also be shown that the MMSE is the same for both equalizers. The intersymbol-interference (ISI) component of the error signal is identical for both equalizers, while the noise component is white for the ADFE and coloured by $\mathbf{w}_f$ for the DFE. Despite the equivalence, identical SNR and timing in both directions is not always guaranteed. The effect of a forward/reverse-link SNR mismatch and the issue of timing in the ADFE system are addressed in later sections.

B. ADFE system training

Training is alternated with data transmission to allow the equalizers to adapt to changing channel conditions. Training and data transmission are composed of four steps:

1. *Reverse-link training:* The portable transmits a training sequence, which the base station uses to adapt its synchronization, AGC, and DFE coefficients.
2. *Reverse-link data transmission:* The portable transmits a frame of data, which is equalized by the DFE and detected by the base station.
3. *Forward-link training:* The base station transfers the FF coefficients of the DFE directly to the FF of the ADFE. A gain factor is incorporated to achieve a desired level of output power. The base transmits a training signal, which is pre-equalized by the FF of the ADFE. The training sequence may be designed for reduced complexity at the portable [12]. The portable estimates the combined impulse response of the channel and FF and computes the FBF coefficients.
4. *Forward-link data transmission:* The base transmits a frame of data, which has been pre-equalized by the FF of the ADFE to reduce precursor ISI in the received signal, and the FBF at the portable cancels postcursor ISI. Equalization complexity at the portable is reduced to channel identification, simple synchronization, and simple implementation of an FBF.

Table 1
Computational complexity of equalization systems

System	Base station			Portable		
	Multiply	Add	Mod	Multiply	Add	Mod
DFE	$4N_f$	$4N_f + 4N_b$	—	$4N_f$	$4N_f + 4N_b$	—
TH-FF	$8N_f + 4N_b$	$8N_f + 8N_b$	2	—	—	2
ADFE	$4N_f$	$8N_f + 4N_b$	—	—	$4N_b$	—

C. Computational complexity

The principal advantage of the ADFE system lies in the distribution of computational complexity. In this section, the complexity of training and equalization of the ADFE system is addressed. Comparison is made with the corresponding DFE and TH-FF systems.

1. *Training complexity*

In the training mode the equalizers of the ADFE system at the base use a recursive least squares (RLS) algorithm. Operations required for training an N-tap equalizer range from $O(N)$ to $O(N^2)$ per training symbol [13] and are the same for DFE, TH-FF and ADFE. The portable uses least-squares channel estimation (LSCE) in the training mode. If a sequence with ideal correlation properties is used, the portable requires only one signed complex addition per training symbol per tap. For other sequences there is a slight decrease in accuracy and/or increase in complexity [12].

2. *Equalization complexity*

For the comparison, we assume QPSK modulation. The figures given are the number of real multiplications, additions and modulo operations per QPSK symbol. The FF and FBF of the ADFE and the FBF of the DFE are implemented with signed additions replacing multiplications. Multiplications are the most expensive of these operations in terms of execution time and/or hardware complexity; the modulo and addition operations are roughly equivalent. Each equalizer has N_f FF taps and N_b FBF taps.

Table 1 compares the number of operations required at the base station and portable for three equalization systems. The first is a symmetric (DFE) system with DFEs at the portable and base station for the forward and feedback links, respectively. The other two systems use a DFE for the reverse link while using a TH-FF precoder and ADFE, respectively, for the forward link. The number of real operations required to equalize one QPSK symbol on each of the forward and reverse links is tabulated. The complexity of the DFE system is divided evenly between base station and portable. While the TH-FF system achieves a higher degree of asymmetry, the ADFE system has a looser AGC requirement, which further simplifies the portable.

D. SNR mismatch

The forward-link CIR is identical to the reverse-link CIR, due to the assumption of reciprocity and identical timing phase. However, the forward-link SNR may differ from that of the reverse link due to differing transmit powers and noise sources. Thus, the FF of the ADFE is characterized for a different SNR than that to which it would be applied. The following scenarios explain the SNR mismatch:

- *Reverse link:* The DFE coefficients ($\mathbf{w}_{\text{DFE}}$) are determined for the reverse link under one SNR.
- *Forward link:* The base station transfers the reverse-link FF of $\mathbf{w}_{\text{DFE}}$ directly to the FF of the ADFE. The portable determines the FBF of the ADFE under a different SNR. For transmit powers normalized to unity, the difference in SNR is reflected entirely in the noise power.

The resulting forward-link MSE (J_{ADFE}) may be expressed in terms of the coefficient error, $\mathbf{w}_{\text{ADFE}} - \mathbf{w}_{\text{DFE}}$ [13], as in (7):

$$J_{\text{ADFE}} = J_{\text{min,ADFE}} + (\mathbf{w}_{\text{ADFE}} - \mathbf{w}_{\text{DFE}})^T \times \left(\mathbf{R} + \sigma^2_{v,\text{ADFE}}\mathbf{D}\right)(\mathbf{w}_{\text{ADFE}} - \mathbf{w}_{\text{DFE}}). \quad (7)$$

If $\mathbf{w}_{\text{ADFE}}$ is close to $\mathbf{w}_{\text{DFE}}$, as may be expected if $\sigma^2_{v,\text{ADFE}}$ and $\sigma^2_{v,\text{DFE}}$ are both small, then the MSE penalty will also be small. The values of the forward- and reverse-link MSE may also be expressed in terms of the noise variance, as in (8):

$$J_{\text{ADFE}} - J_{\text{min,DFE}} = \left(\sigma^2_{v,\text{ADFE}} - \sigma^2_{v,\text{DFE}}\right)\mathbf{w}^T_{\text{DFE}}\mathbf{D}\mathbf{w}_{\text{DFE}}. \quad (8)$$

If the forward-link SNR exceeds the reverse-link SNR (i.e., $\sigma^2_{v,\text{ADFE}} < \sigma^2_{v,\text{DFE}}$), then

$$J_{\text{min,ADFE}} < J_{\text{ADFE}} < J_{\text{min,DFE}}, \quad (9)$$

and the forward-link MSE performance exceeds that of the reverse link.

E. Fractionally spaced ADFE

1. *Reverse link*

The DFE may incorporate a fractionally spaced (FS) FF to improve performance or reduce synchronization complexity. It would also allow the FF to independently manipulate the frequency response of the excess bandwidth [14]. The FS FF may require more taps than a symbol-spaced (SS) FF.

2. *Forward link*

Directly characterized by the FF of the DFE, the FF of the ADFE may also be implemented with fractional spacing. The synchronization advantages of the FSE would be lost in the forward link because the portable must establish synchronization independent of the base station. However, the benefit of advantageous shaping of the excess bandwidth of the transmitted signal would be retained. In any case, once the FS FF is obtained for the DFE, it is simpler to re-use it for the ADFE. Although the forward-link FBF operates with symbol spacing, a fractionally spaced CIR estimate may be used to combine synchronization and training. The ensuing relaxation in synchronization requirements might offset the increased complexity of the estimation.

3. *MSE analysis for fractionally spaced ADFE*

The MSE analysis of a DFE or ADFE may be extended to fractional spacing with only some minor changes to the notation and results. Analysis of an FSE is complicated by the need to account for different sampling periods; the symbol period, T_s; the sample period, T_{eq}, of the fractionally spaced FF; and fractionally spaced signals. In this analysis, all signals and filters (except the FBF) are represented with a sample period T_{eq}. Signals that are defined at intervals of T_s are upsampled and zero-padded. Some of the vectors and matrices are redefined to accommodate the combination of T_{eq} and T_s spacing. In this case, the expression $\alpha \equiv \beta(\bmod s)$ implies that $\alpha = \beta + Ks$, where K is an arbitrary integer and $s = T_s/T_{eq}$ is a positive integer. Redefine the signal components as

$$a(n) = \begin{cases} \pm 1, & n \equiv 0(\bmod s) \\ 0, & \text{otherwise} \end{cases},$$
$$\mathbf{d}(n-s) = \left[d(n-s) \;\; d(n-2s) \;\; \cdots \;\; d(n-N_b s)\right]^T, \quad (10)$$
$$y(n) = \mathbf{h}^T\mathbf{A}(n)\mathbf{w}_f + \mathbf{w}_v^T\mathbf{v}(n) + \mathbf{w}_b^T\mathbf{d}(n-s).$$

The MMSE weight vector is given by

$$\mathbf{w}_{\text{MMSE}} = \left(\mathbf{R} + \sigma_v^2\mathbf{D}\right)^{-1}\mathbf{p}, \quad \mathbf{w} = \begin{bmatrix}\mathbf{w}_f \\ \mathbf{w}_b\end{bmatrix}, \quad (11)$$

where

$$\mathbf{R} = \begin{bmatrix}\mathbf{R}_1 & \mathbf{R}_3 \\ \mathbf{R}_3^T & \mathbf{I}_{Nb}\end{bmatrix}, \quad \mathbf{p} = \begin{bmatrix}\mathbf{r}_2 \\ \mathbf{0}_{Nb}\end{bmatrix}.$$

The diagonal matrix $\mathbf{D}$ and the vector $\mathbf{r}_2$ are the same as for the symbol-spaced case. The matrices $\mathbf{R}_1$ and $\mathbf{R}_3$ have elements given, respectively, by (12) and (13):

$$\mathbf{R}_1(i,j) = \sum_{\substack{k=0 \\ k+i-\Delta\equiv 1(\bmod s)}}^{N_h-1} h(k)h(k-i+j), \quad i,j = 1,2,\ldots,N_f, \quad (12)$$

$$\mathbf{R}_3(i,j) = h(js - i + \Delta + 1), \quad i = 1,2,\ldots,N_f, \; j = 1,2,\ldots,N_b. \quad (13)$$

As before, the MMSE and MMSE coefficients are identical for the DFE and the ADFE, and the error signal $e(n)$ is coloured for the DFE and white for the ADFE.

IV. Markov model of error propagation

Due to error propagation, analysis of the bit-error-rate (BER) performance is very difficult to carry out for a DFE system [15]. This section presents an exact method of modelling error propagation in the ADFE. It also leads to interesting results for the correlation of decision errors.

A. Decision errors in the DFE

A decision error occurs when the output of the decision device differs from the desired symbol. Sources of decision errors are additive noise, precursor ISI, and postcursor ISI and error propagation. The noise at the output of the forward filter is Gaussian and coloured. The precursor ISI is non-Gaussian and arises from imperfect cancellation by the forward filter. Non-ideal values of the feedback coefficients or insufficient number of feedback taps give rise to non-Gaussian postcursor ISI. Furthermore, a decision error will contribute to postcursor ISI, which can cause error propagation. Error propagation complicates the error performance analysis considerably.

Analysis of DFE decision errors may be simplified by assuming that the noise input to the decision device is Gaussian and white, that there is no precursor ISI, and that the feedback taps are of sufficient number and exact values to eliminate postcursor ISI [16]–[18]. Austin [18] used a finite discrete Markov process to model the effect of error propagation and predict the BER of a DFE system. Subsequent authors [16], [19] have used a reduced state representation of error propagation to derive upper bounds on the probability of error. Previous modelling of the DFE feedback filter by a Markov process does not accurately model residual precursor ISI and noise filtering in all cases [17].

B. Error propagation in the ADFE

The Markov state model may be applied to the ADFE without any need for assumptions regarding the statistics of filtered noise or precursor elimination. Although not considered in this paper, the assumptions of precursor elimination and ideal feedback coefficients could be used to reduce the number of states.

For simplicity of analysis only, BPSK is assumed, and all signals are assumed to be real. Other modulations may be represented with complex arithmetic, with an increased number of states. The variable $d(n)$ is the transmitted symbol. The decoded symbol is defined in (14):

$$\hat{d}(n) = \begin{cases} -1, & y(n) \le 0 \\ +1, & y(n) > 0 \end{cases}. \quad (14)$$

The signal $y(n)$ (see (4)) is Gaussian with mean and variance given, respectively, by

$$m_y = \sum_{k=0}^{N_q-1} q(k)d(n+\Delta-k) + \sum_{k=1}^{N_b} w_b(k)\hat{d}(n-k) \quad (15)$$

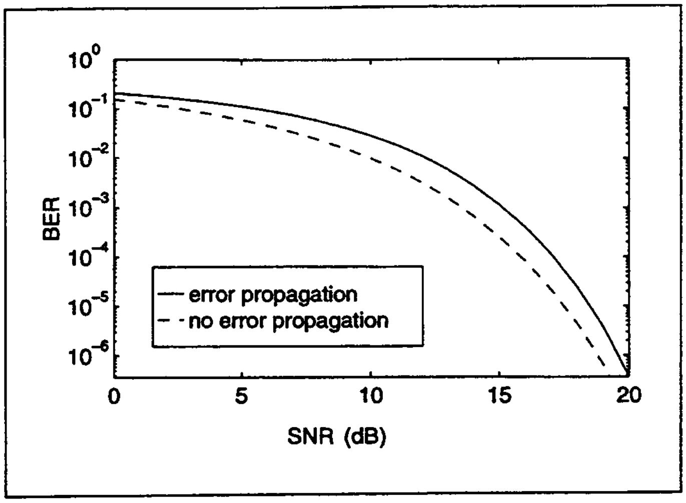

Figure 3: *Markov model and simulation results, with and without error propagation.*

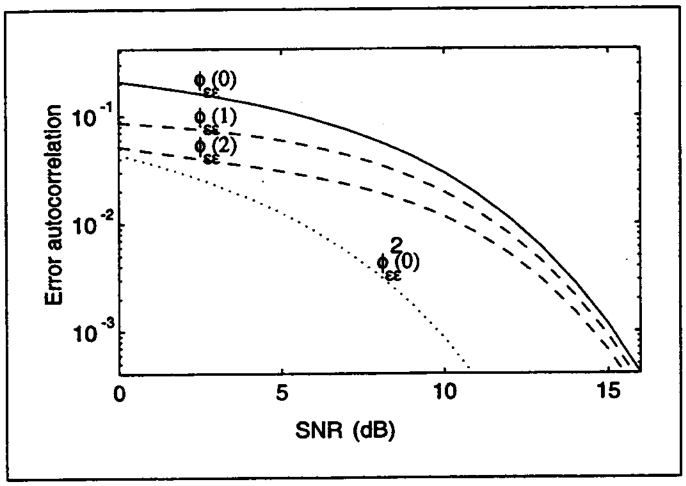

Figure 4: *Autocorrelation of error-event function.*

and $\sigma_y^2 = E[v^2(n)]$. The j-th state of the system may be defined by (16):

$$S_j = \begin{cases} d(n-\Delta-k), & k = 0,1,\ldots,N_q-1 \\ \hat{d}(n-k), & k = 1,2,\ldots,N_b \end{cases}, \tag{16}$$

where N_q is the order of the pre-equalizer filter convolved with the channel impulse response. For BPSK, the number of states is $2^{N_q+N_b}$, each having four nonzero transition probabilities. For example, the nonzero transition probability for the state $\{\hat{d}(n) = -1,\ d(n+\Delta+1) = -1 \mid S_i\}$ is given by (17):

$$\begin{aligned} P_{ij} &= P\left(\hat{d}(n) = -1, d(n+\Delta+1) = -1 \mid S_i\right) \\ &= \frac{1}{2}P\left(y(n) \leq 0 \mid S_i\right). \end{aligned} \tag{17}$$

The four nonzero transition probabilities are given by (18) and (19):

$$P\left(\hat{d}(n) = -1, d(n+\Delta+1) = \pm 1 \mid S_i\right) = \frac{1}{4}\mathrm{erfc}\left(\frac{m_y}{\sqrt{2}\sigma_y}\right), \tag{18}$$

$$P\left(\hat{d}(n) = +1, d(n+\Delta+1) = \pm 1 \mid S_i\right) = \frac{1}{4}\mathrm{erfc}\left(\frac{-m_y}{\sqrt{2}\sigma_y}\right). \tag{19}$$

The transition probabilities are used to compute the state transition matrix. The state probabilities and BER are in turn computed from the transition matrix [18]. The BER includes the effects of ISI, noise, and error propagation. For this study the channel is $\mathbf{h} = [1,2,1]^T$; the filter orders are $N_f = 3$, $N_b = 1$; and the characterization is MMSE. Fig. 3 shows the BER of the ADFE with and without error propagation. As would be expected, the SNR penalty to compensate for error propagation is smallest at higher values of the SNR. Results show a perfect match between Markov modelling and simulation.

C. Error-event correlation

To gain further insight into the effects of error propagation, we examine the error-event correlation. Define the error-event function, $\varepsilon(n)$, as in (20):

$$\varepsilon(n) = \begin{cases} 0, & \hat{d}(n) = d(n) \\ 1, & \hat{d}(n) \neq d(n) \end{cases}. \tag{20}$$

The error-event autocorrelation function, $\phi_{\varepsilon\varepsilon}(k)$, is defined by (21):

$$\phi_{\varepsilon\varepsilon}(k) = E[\varepsilon(n)\varepsilon(n-k)] = P(\varepsilon(n) = 1, \varepsilon(n-k) = 1). \tag{21}$$

Two properties are identified: (i) the zeroth-lag autocorrelation is the average probability of bit error, and (ii) if errors are independent, then the autocorrelation at nonzero lags is the probability of error squared. The second property may be used to examine the degree of correlation between errors. If the autocorrelation is close to the value of the error probability squared, then the errors are nearly independent.

Fig. 4 shows error-event autocorrelation curves for up to three consecutive errors. At lower SNRs, the probability of a single error is significantly greater than that of two or three consecutive errors. At higher SNRs, these probabilities decrease sharply with increasing SNR, and the difference between the probabilities of one, two and three errors is significantly reduced.

V. Effect of non-idealities on BER performance

The simplified model in the previous sections omits non-idealities. It may be used to provide an indication of initial performance only. This section examines the effect of non-idealities on BER performance. In order to limit complexity, only one non-ideality is considered at a time. The non-idealities examined are the effect of timing error, SNR mismatch, adaptive training and finite precision arithmetic. The accuracy of the results is limited by the accuracy and completeness of the models.

A. SNR mismatch

In an ADFE system, the forward link is pre-equalized by the FF, which is determined from the reverse-link CIR and SNR. While the principle of reciprocity may hold for the forward- and reverse-link CIR, the SNR will differ. This SNR mismatch is investigated by determining the performance of the ADFE at different execution (forward link) and characterization (reverse link) SNR. For the simulation, the channel is $\mathbf{h} = [1,2,1]^T$; the filter orders are $N_f = 4$, $N_b = 1$; and modulation is BPSK.

Figs. 5 and 6 illustrate the effect of the SNR mismatch on MSE and BER performance. As expected, the MMSE is obtained when the characterization SNR is greater than the execution SNR. Fig. 6 illustrates the discrepancy between MMSE and minimum probability of error criteria. For the given CIR, it would appear to be advantageous to characterize at a fixed SNR of about 10 dB, regardless of the execution SNR. Further experiments, however, reveal that the effect of SNR mismatch varies considerably with CIR and equalizer. Some channels have good BER performance at any training SNR above about 10 dB, while others do not. This would suggest the need for analysis to extract the underlying principles and derive algorithms for enhancing performance of real systems; however, such an investigation is beyond the scope of this paper. Both the ADFE and the DFE exhibit a similar sensitivity to SNR mismatch.

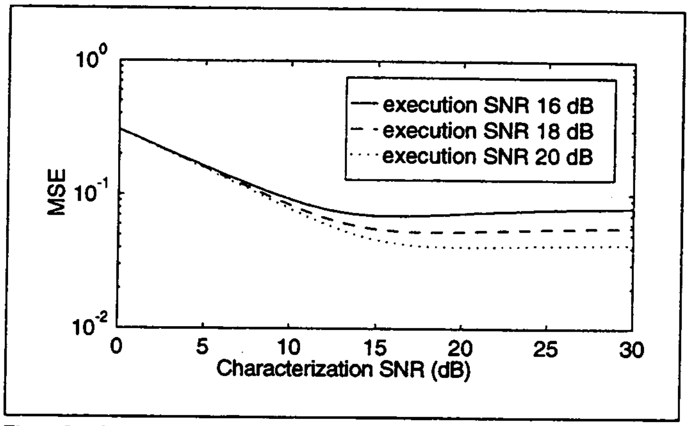

Figure 5: *MSE performance of ADFE with SNR mismatch.*

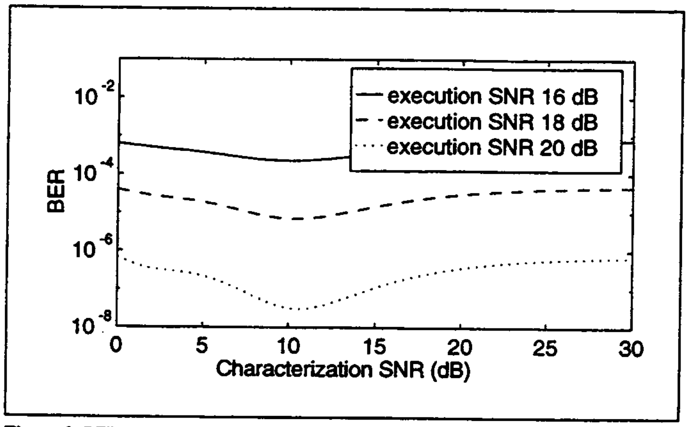

Figure 6: *BER performance of ADFE with SNR mismatch.*

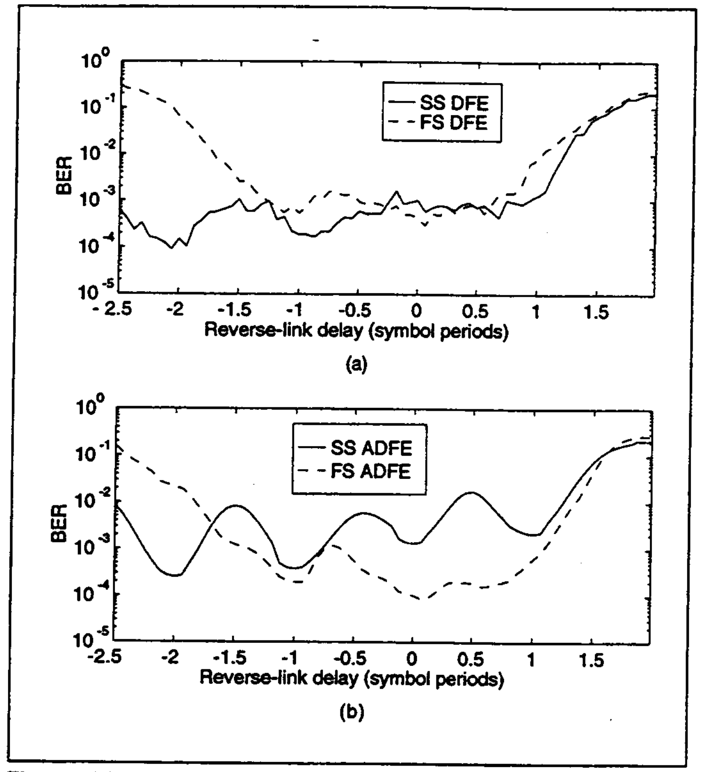

Figure 7: *BER performance: (a) timing sensitivity of reverse link (DFE); (b) joint timing sensitivity of forward link (ADFE).*

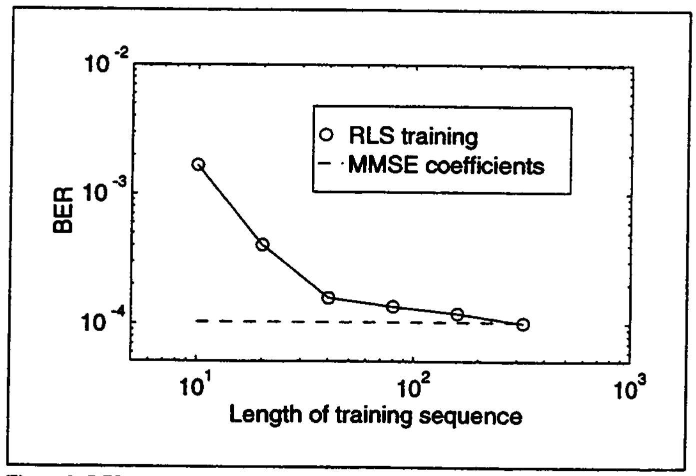

Figure 8: *DFE adaptive RLS training.*

B. Sensitivity to timing error

Timing (synchronization) involves both the timing phase and choice of main ray of the CIR. This section investigates the effect of timing error on the reverse and forward links of the ADFE system for equalizers with a T_s-spaced (TSE) and $T_s/2$-spaced (FSE) FF. Variable timing is obtained from the CIR by interpolation with a raised-cosine or square-root raised-cosine pulse shape followed by resampling. The received signal energy before (down) sampling is maintained constant to simulate the effect of a constant SNR at the receiver input. Thus, the SNR after sampling will vary with the timing phase.

1. *Reverse link (DFE)*

In the ADFE system, the base receiver establishes an appropriate timing with the reverse-link signal. The choice of timing will affect the reverse-link performance. For this study, $\mathbf{h} = [1, 2, 1]$, SNR $= 15$ dB, $N_f = 5$, $N_b = 1$, and modulation is BPSK. Fig. 7(a) illustrates the effect of varied timing on the BER of the reverse link, for a DFE with an SS FF and an FS FF. For the selected channel, the DFE FF is able to synthesize the appropriate timing over a fairly wide range of delays. There is no apparent advantage in timing sensitivity from using an FS FF. However, it would be rash to draw a general conclusion without investigation of different channels, SNRs, and filter lengths.

2. *Joint forward/reverse-link timing error*

On the forward link of the ADFE system, the task of synchronization is shared between the transmitter (base) and receiver (portable). The receiver must synchronize to a main ray that is predetermined by the FF at the transmitter. Since the forward-link receiver has no FF, there is no opportunity to synthesize a delay characteristic, and very little timing error can be tolerated. The timing sensitivity might be reduced by employing fractionally spaced channel estimators. The increased complexity might be compensated for by an improvement in performance and simplification of synchronization.

Joint timing error refers to the effect of timing error from the reverse link on the forward link. Timing error during reverse-link training of the DFE is transferred to the forward link through re-use of the FF. The FF is characterized according to the CIR, timing phase, and delay established in reverse-link training, and is subsequently made part of the effective forward-link channel for the purposes of data transmission and timing recovery. A poor choice of reverse-link timing will be reflected in the forward-link performance.

Fig. 7(b) illustrates the effect of reverse-link timing on the forward-link performance, for the same simulation parameters as in Fig. 7(a). The FSE seems to impart the benefit of reduced sensitivity of the forward link to reverse-link timing error within $\pm T_s$.

C. Adaptive training

The ADFE system uses an RLS to characterize the DFE and the ADFE FF at the base, while LSCE is used to characterize the ADFE FBF at the portable. Since these forms of training only approximate the

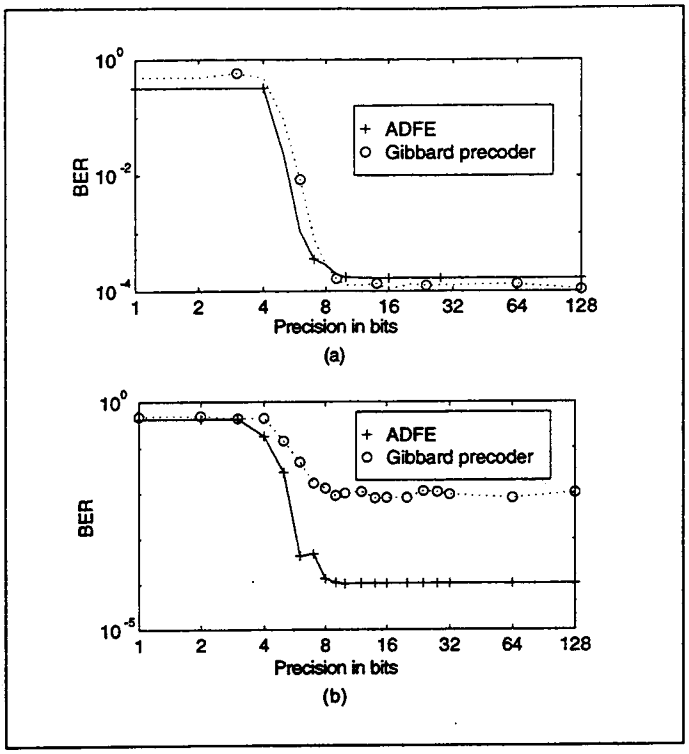

Figure 9: *Finite precision BER performance.*

MMSE solution, it is valuable to compare the resulting performance with MMSE characterizations.

Fig. 8 compares equalizer BER performance with MMSE adaptive training and characterization. For this study, $\mathbf{h} = [1, 2, 1]^T$, SNR = 17 dB, $N_f = 4$, $N_b = 1$ and modulation is BPSK. While MSE is often used to evaluate equalizer convergence, the BER is more indicative of actual performance. It appears that equalization with adaptive training is able to approximate the BER performance of MMSE coefficients, provided that the training sequence is of sufficient length.

D. Finite precision

The accuracy of the equalizer output in the ADFE system is affected by the precision of the input data and the internal arithmetic operations. Simulation is used because the relationship between numerical precision and BER performance is difficult to analyze. The effect of finite precision arithmetic was modelled by including a nonlinear and memoryless quantization operation. The quantizer, represented by $Q(\cdot)$, operates on the input, output, operands and all products. If an FIR filter has coefficients $w(k)$, an input $x(n)$, and output $y(n)$, the effect of finite precision is modelled by (22):

$$\begin{aligned} w_Q(k) &= Q[w(k)], \\ x_Q(n) &= Q[x(n)], \\ y_Q(n) &= Q\left[\sum_{k=0}^{N_w-1} w_Q(k)x_Q(n-k)\right]. \end{aligned} \tag{22}$$

Performance was compared for a large number of channels. Fig. 9 illustrates the performance of the ADFE and the TH-FF [2] schemes with finite precision arithmetic for two channels. The common parameters are $N_f = 3$, $N_b = 2$; modulation is BPSK. For Fig. 9(a), $\mathbf{h} = [1, 2, 2, 1]$ and SNR = 24 dB, and for Fig. 9(b), $\mathbf{h} = [-1, 2, 2, -1]$ and SNR = 11 dB. Performance for both ADFE and TH-FF is almost identical at low precision ($\leq$4 bits) for all the channels investigated. For less severe channels, both systems performed satisfactorily at higher than 8-bit precision, and both seemed to be insensitive to precision in that range (Fig. 9(a)). Whereas the ADFE system remained insensitive, the TH-FF system was sensitive to the severity of the channel and performed poorly on harsh channels (Fig. 9(b)).

Extensive simulation studies were carried out, and the results indicate that performance curves for the DFE and the TH-FF are identical with those presented here for the ADFE. The only significant difference observed was the sensitivity to finite precision implementation, which is illustrated in Fig. 9. The identical performance for the ADFE, DFE and TH-FF is not surprising because the only difference is in the placement of the various components of the DFE structure. The high sensitivity of the TH-FF to finite precision is due to the fact that its feedback filter operates on non-quantized inputs, which may cause quantization and round-off errors. Such errors may, in turn, cause instability.

VI. Summary and conclusions

This paper has presented a new equalization structure, the asymmetric decision feedback equalizer (ADFE), and a system for asymmetric equalization (the ADFE system) for full-duplex indoor wireless communication. The ADFE was analyzed by means of MSE and BER performance. The BER analysis was facilitated by application of a finite discrete Markov process to model the effects of noise, residual precursor ISI, and error propagation. In addition, information on error propagation was extracted from the state transition matrix and an error-event correlation function was defined. One caveat for the Markov model is that it may yield unreasonable results, such as a negative BER when the expected BER is small ($<10^9$, say). This is probably due to the limited (albeit high) numerical precision used to initialize and solve the state transition matrix.

The effects of SNR mismatch, timing error, adaptive training, and finite precision arithmetic on BER were determined by Markov modelling and simulation.

Appendix: Derivation of the MSE for symbol-spaced ADFE

The mean square error is defined by

$$J = E\left[e^2(n)\right], \tag{A-1}$$

$$J = E\left[\left(d(n) - u(n) - \mathbf{w}_v^T\mathbf{v}(n) - \mathbf{w}_b^T\mathbf{d}_{Nb}(n-1)\right)^2\right], \tag{A-2}$$

$$\begin{aligned} J = {} & E\left[d^2(n)\right] + \mathbf{w}_f^T E\left[\mathbf{A}^T(n)\mathbf{h}\mathbf{h}^T\mathbf{A}(n)\right]\mathbf{w}_f \\ & + \mathbf{w}_b^T E\left[\mathbf{d}_{Nb}(n-1)\mathbf{d}_{Nb}^T(n-1)\right]\mathbf{w}_b - 2\mathbf{w}_f^T E\left[d(n)\mathbf{A}^T(n)\right]\mathbf{h} \\ & - 2\mathbf{w}_f^T E\left[\mathbf{A}^T(n)\mathbf{h}\mathbf{d}_{Nb}^T(n-1)\right]\mathbf{w}_b + \mathbf{w}_v^T E\left[\mathbf{v}(n)\mathbf{v}^T(n)\right]\mathbf{w}_v. \end{aligned}$$

The following correlation matrices may be used to simplify the above expression:

$$\mathbf{R}_1 = E\left[\mathbf{A}^T(n)\mathbf{h}\mathbf{h}^T\mathbf{A}(n)\right] = \begin{bmatrix} r_{hh}(0) & r_{hh}(1) & \cdots r_{hh}(N_f-1) \\ r_{hh}(1) & r_{hh}(0) & \cdots r_{hh}(N_f-2) \\ \vdots & \vdots & \ddots \quad \vdots \\ r_{hh}(N_f-1) & r_{hh}(N_f-2) & \cdots \quad r_{hh}(0) \end{bmatrix}, \tag{A-3}$$

$$r_{hh}(k) = \sum_{j=0}^{Nh-k-1} h(j)h(j+k), \tag{A-4}$$

$$\mathbf{r}_2 = E\left[d(n)\mathbf{A}^T(n)\right]\mathbf{h} = \begin{bmatrix} h(\Delta) \\ h(\Delta-1) \\ \vdots \\ h(\Delta-N_f+1) \end{bmatrix}, \tag{A-5}$$

$$\mathbf{R}_3 = E\left[\mathbf{A}^T\mathbf{h}\mathbf{d}^T(n-1)\right], \tag{A-6}$$

$$\mathbf{R}_3 = \begin{bmatrix} h(\Delta+1) & h(\Delta+2) & \cdots & h(\Delta+N_b) \\ h(\Delta) & h(\Delta+1) & \cdots & h(\Delta+N_b-1) \\ \vdots & \vdots & \ddots & \vdots \\ h(\Delta-N_f+2) & h(\Delta-N_f+3) & \cdots & h(\Delta-N_f+N_b+1) \end{bmatrix}, \tag{A-7}$$

$$J = 1 + \mathbf{w}_f^T\mathbf{R}_1\mathbf{w}_f + \sigma_v^2\mathbf{w}_v^T\mathbf{w}_v + \mathbf{w}_b^T\mathbf{I}_{Nb}\mathbf{w}_b - 2\mathbf{w}_f^T\mathbf{r}_2 - 2\mathbf{w}_f^T\mathbf{R}_3\mathbf{w}_b. \tag{A-8}$$

For both the DFE and the ADFE, the condition $\mathbf{w}_v^T\mathbf{w}_v = \mathbf{w}_f^T\mathbf{w}_f$ holds:

$$J = 1 + \mathbf{w}_f^T\left(\mathbf{R}_1 + \sigma_v^2\mathbf{I}_{Nf}\right)\mathbf{w}_f + \mathbf{w}_b^T\mathbf{I}_{Nb}\mathbf{w}_b - 2\mathbf{w}_f^T\mathbf{r}_2 - 2\mathbf{w}_f^T\mathbf{R}_3\mathbf{w}_b. \tag{A-9}$$

The expression for J is rendered more compact by combining matrices as follows:

$$\mathbf{w} = \begin{bmatrix}\mathbf{w}_f \\ \mathbf{w}_b\end{bmatrix}, \quad \mathbf{R} = \begin{bmatrix}\mathbf{R}_1 & \mathbf{R}_3 \\ \mathbf{R}_3^T & \mathbf{I}_{Nb}\end{bmatrix}, \quad \mathbf{p} = \begin{bmatrix}\mathbf{r}_2 \\ \mathbf{0}_{Nb}\end{bmatrix}, \tag{A-10}$$

$$J = 1 + \mathbf{w}^T\left(\mathbf{R} + \sigma_v^2\mathbf{D}\right)\mathbf{w} - 2\mathbf{w}^T\mathbf{p}. \tag{A-11}$$

The matrix $\mathbf{D}$ is diagonal with elements given by

$$D_{ii} = \begin{cases} 1, & i = 1, 2, \ldots, N_f \\ 0, & i = N_f+1, N_f+2, \ldots, N_f+N_b \end{cases}. \tag{A-12}$$

Acknowledgements

This work was supported by TRLabs and by the Natural Sciences and Engineering Research Council (NSERC) of Canada.

References

[1] C.L.B. Despins, D.D. Falconer, and S.A. Mahmoud, "Compound strategies of coding, equalization, and space diversity for wideband TDMA indoor wireless channels," *IEEE Trans. Veh. Tech.*, vol. 41, no. 4, pp. 369–379, Nov. 1992.

[2] M.R. Gibbard, A.B. Sesay, and L. Strawczynski, "Asymmetric equalization structure for broadband indoor wireless data communications," in *Proc. 6th Int. Conf. Wireless Communications*, vol. 2, Calgary, Alta., July 11–13, 1994, pp. 521–535.

[3] H. Sari and G. Karam, "Asymmetric baseband equalization," *IEEE Trans. Comm.*, vol. 36, no. 9, pp. 1073–1078, Sept. 1988.

[4] W.E. Stephens, H. Samueli, and G. Cherubini, "Guest editorial: Copper wire access technologies for high performance networks," *IEEE J. Select. Areas Comm.*, vol. 13, no. 9, pp. 1537–1539, Dec. 1995.

[5] W. Zhuang, W.A. Krzymien, and P.A. Goud, "Adaptive channel precoding for personal communications," *Electron. Lett.*, vol. 30, pp. 1570–1571, Sept. 1994.

[6] W. Zhuang and V. Huang, "Nonlinear phase precoding for personal communications," *Electron. Lett.*, vol. 30, pp. 2010–2011, Nov. 1994.

[7] L.J. Karr, "Polled data network auto-equalizer system and method," U.S. Patent No. 4969162, issued Nov. 6, 1990.

[8] G.J. Korevaar, "Terminal arrangement for a duplex transmission system," U.S. Patent No. 4535433, issued Aug. 13, 1985.

[9] H. Harashima and H. Miyakawa, "Matched-transmission technique for channels with intersymbol interference," *IEEE Trans. Comm.*, vol. 20, no. 4, pp. 774–780, Aug. 1972.

[10] M. Tomlinson, "New automatic equalizer employing modulo arithmetic," *Electron. Lett.*, vol. 7, pp. 138–139, Mar. 1971.

[11] T.A. Freeburg, "Enabling technologies for wireless in-building network communications—Four technical challenges, four solutions," *IEEE Comm. Mag.*, vol. 29, no. 4, pp. 58–64, Apr. 1991.

[12] S.N. Crozier, D.D. Falconer, and S.A. Mahmoud, "Least sum of squared errors channel estimation," *Proc. IEE-F*, vol. 138, no. 4, pp. 371–378, Aug. 1991.

[13] S. Haykin, *Adaptive Filter Theory*, Englewood Cliffs, N.J.: Prentice Hall, 1991.

[14] S.H. Qureshi, "Adaptive equalization," *Proc. IEEE*, vol. 73, no. 9, pp. 1349–1387, Sept. 1985.

[15] C.A. Belfiore and J.H. Park Jr., "Decision feedback equalization," *Proc. IEEE*, vol. 67, no. 8, pp. 1143–1156, Aug. 1979.

[16] S.A. Altekar and N.C. Beaulieu, "Upper bounds to the error probability of decision feedback equalization," *IEEE Trans. Inform. Theory*, vol. 39, no. 1, pp. 145–156, Jan. 1993.

[17] P. Monsen, "Adaptive equalization of the slow fading channel," *IEEE Trans. Comm.*, vol. 22, no. 8, pp. 1064–1075, Aug. 1974.

[18] M.E. Austin, "Decision-feedback equalization for digital communication over dispersive channels," MIT Research Lab. Electronics, Cambridge, Mass., Tech. Rep. 461, Aug. 1967.

[19] D.L. Duttweiler, J.E. Mazo, and D.G. Messerschmitt, "An upper bound to the error probability in decision-feedback equalization," *IEEE Trans. Inform. Theory*, vol. 20, no. 4, pp. 490–497, July 1974.